International Journal of Mass Spectrometry 179/180 (1998) 253–260

Energy partitioning following the infrared photofragmentation of $SF_6.(C_6H_6)^+$ cluster ions

S. Atrill, A.J. Stace*

School of Chemistry, Physics and Environmental Science, University of Sussex, Falmer, Brighton BN1 9QJ, UK

Received 17 April 1998; accepted 14 July 1998

Abstract

Kinetic energy release measurements have been performed following the metastable and infrared photoinduced decay of $SF_6.(C_6H_6)_n^+$ cluster ions. Using a model due to Klots [J. Chem. Phys. 58 (1973) 5364], photofragment kinetic energy releases have been predicted on the assumption that energy from the photon (~950 cm^{-1} deposited into the ν_3 of the SF_6 moiety) is partitioned statistically throughout the cluster ion. However, a comparison between experimental and calculated results suggests that incomplete energy randomisation may be taking place, and a better description of the photofragmentation process is provided on the assumption that the excited vibrational mode undergoes partial relaxation to either the ν_2 or ν_4 modes. The energy difference (~300 cm^{-1}) is then randomised and is reflected in the magnitudes of the measured kinetic energy releases. (Int J Mass Spectrom 179/180 (1998) 253–260) © 1998 Elsevier Science B.V.

Keywords: Infrared photodissociation; Cluster ions; Kinetic energy release

1. Introduction

In two previous publications [1,2], we have shown how the infrared photoexcitation of SF_6-containing cluster ions can lead to incomplete energy transfer between the chromophore (SF_6) and the cluster heat sink. In these experiments, the kinetic energy release associated with the metastable decay of each ion has been recorded and used to establish an internal energy and temperature. The process was then repeated following laser-induced infrared photodissociation, and the new kinetic energy release used to record a temperature increase which in turn was compared with that calculated from a model due to Klots [3]. The examples studied were $SF_6.Ar_n^+$ and $SF_6.(NO)_n^+$ [1,2], and in both cases it was shown that excitation of the ν_3 vibrational mode in SF_6 at 950 cm^{-1} leads to incomplete energy randomization. These observations could be accounted for by assuming that SF_6 undergoes vibrational relaxation from ν_3 to either the ν_2 or ν_4 vibrational levels, and that the energy difference is dissipated to the internal modes of the heat sink. Since the energy separation between the ν_2 and ν_4 modes is only ~30 cm^{-1}, the resolution of the experiment was not sufficient to give a precise identification of the final vibrational state.

In the examples studied thus far, the heat sinks have contained a limited number of internal degrees of freedom. In the experiments reported here we have extended the range of measurements to include the

---

* Corresponding author.

Dedicated to Professor Fulvio Cacace in recognition of his outstanding contributions for many decades to gas-phase ion chemistry and physics.

PII S1387-3806(98)14144-1

system $SF_6.(C_6H_6)_n^+$, which complements the earlier results in that the cluster component now consists of molecules which have large numbers of internal degrees of freedom. However, there is a further reason as to why the $SF_6.(C_6H_6)_n^+$ system is of interest. Following the isolation of a single size of cluster ion, two metastable fragmentation routes are observed [4]

$$SF_6.(C_6H_6)_n^+ \rightarrow SF_6.(C_6H_6)_{n-1}^+ + C_6H_6 \quad (1)$$

$$SF_6.(C_6H_6)_n^+ \rightarrow (C_6H_6)_n^+ + SF_6 \quad (2)$$

The loss of a benzene molecule via reaction (1), is by far the more dominant metastable dissociation process, with intensities six to eight times those observed for the loss of SF_6 [4]. Part of this difference could be attributed to reaction path degeneracy. However, following excitation with an infrared photon from a CO_2 laser, the only photoinduced fragmentation route observed is the loss of SF_6 via reaction (2). This complete reversal of reaction probability is unusual when compared with the pattern of behaviour seen in similar systems studied thus far [4–7]. Only three other mixed cluster ions have been observed to lose SF_6 following photoexcitation, and these very specific examples are: $SF_6.Kr_3^+$ [8], $SF_6.(NO)_3^+$ [6], and $SF_6.(NO)_5^+$ [6]. However, all of these ions also exhibited the same loss channel under conditions of metastable decay.

2. Experimental

Neutral clusters of the form $SF_6.(C_6H_6)_n$ were prepared using the “pick-up” [9] technique on an apparatus that consists of a pulsed supersonic nozzle coupled to a modified double focusing, reverse geometry, high resolution mass spectrometer (VG ZAB-E). Benzene clusters were produced by partly filling a stainless steel reservoir with the liquid (5 cm^3, Aldrich 99.99% spectroscopic grade) and using argon as a carrier gas to transport the vapour into the nozzle assembly. Following collimation through a 1 mm diameter skimmer, the benzene cluster beam entered a flight tube approximately 70 cm long, in which the background pressure had been increased to 10^{-5} mbar through the introduction of SF_6 via a needle valve. A combination of cooling the reservoir with ice together with an argon backing pressure of 35 psi were found to provide the optimum conditions necessary for producing intense $SF_6.(C_6H_6)_n^+$ signals. As in previous studies [4–7], the presence of argon as the carrier gas was found to be essential to the success of the pick-up procedure. It is thought that an important intermediate step is the formation of mixed $(C_6H_6)_n.Ar_m$ clusters which then undergo the exchange reaction

$$(C_6H_6)_n.Ar_m + SF_6 \rightarrow SF_6.(C_6H_6)_n.Ar_k + (m-k)Ar \quad (3)$$

with the argon acting as an energy sink in the exchange reaction.

Ionisation was achieved using 70 eV electrons and at that stage any remaining argon atoms are assumed to be lost from the mixed cluster ions. For this series of experiments an accelerating voltage of 7 kV was used to extract ions from the source. The resolution of the mass spectrometer was increased to the highest practical level while still maintaining a level of signal adequate for quantitative measurements. In this way, any contribution that the spread in parent ion kinetic energy makes to the metastable and laser-induced kinetic energy profiles could be kept to a minimum. Typically, the parent ion kinetic energy spread [full width at half maximum (FWHM)] was of the order of 1.5–2.0 eV in the laboratory-frame, which led to a parent ion contribution of $<10\%$.

The masses of any ionic photofragments were determined using the electrostatic analyser in the mass-analysed ion kinetic energy spectra (MIKES) mode [10]. To separate laser-induced fragmentation processes from either metastable decay or collision-induced dissociation (CID), the laser beam was modulated at half the nozzle frequency and foreground–background subtraction performed on photofragment signals. Two data collection techniques were employed: photodissociation and unimolecular (metastable) decay signals at a single kinetic energy were recorded using gated photon counting via a scintillation (Daly) ion detector; mass spectra were recorded using phase-sensitive detection in conjunction with analogue output from the ion detection system. To keep CID processes to a minimum, the background pressure in the flight tube was maintained at 6×10^{-9} mbar. Photodissociation signals were between 10^3 and 10^5 counts $\min^{-1}$ against a background signal of $<10^2$ counts $\min^{-1}$. A typical error bound on photofragmentation signal intensity at a given laboratory frame kinetic energy is ±5%. Power-dependence studies showed that most photodissociation steps were single photon events, and none of the processes discussed here showed any dependence on the angle of polarisation of the laser radiation.

For each mass-selected cluster ion, the width and intensity of any underlying metastable or unimolecular decay product was recorded at the same time as the laser signal. Because the average kinetic energy release associated with each metastable process is used to define the initial temperature of a cluster ion, the simultaneous recording of both signals served to reduce any uncertainty imposed by instrumental drift during the 2–3 h it took to record each result. As a result of the very weak metastable signal observed for the loss of SF_6 from each cluster ion (as opposed to the metastable loss of benzene), the corresponding kinetic energy profiles exhibit some noise. This was accentuated as a result of the increase in mass spectral resolution required by this particular series of experiments.

3. Calculation of cluster temperature

From earlier work by Klots [3], the relationship between the excess energy of a cluster ion above threshold, (E^*) and a temperature (T^*) for the dissociating products can be derived from statistical mechanics as follows:

$$E^* = \frac{(R-1)}{2} k_B T^* + k_B T^* + \sum_i \frac{h\nu_i}{[\exp(h\nu_i/k_B T^*) - 1]}, \tag{4}$$

where R is the number of rotational degrees of freedom in the reaction products and the summation is performed over all vibrational frequencies of the products (with ν_i being the harmonic frequency of the ith mode, and k_B is Boltzmann's constant). In some respects, T^* could be considered as the temperature of the reaction transition state [3]. A second relationship defines the connection between T^* and the average kinetic energy release (ε_t) as [3]

$$\varepsilon_t = k_B T^*. \tag{5}$$

Thus a measurement of ε_t can establish T^*, which in turn can be used to calculate E^* from Eq. (4). If the "temperature" of the cluster ion is now increased through the addition of an infrared photon, there will be a new excess energy (namely $E^* + E_{ph}$) which can be equated with an increase in temperature from T to $T + \Delta T$ as follows:

$$E^* + E_{ph} = \frac{(R-1)}{2} k_B\{T^* + \Delta T\} + k_B\{T^* + \Delta T\} + \sum_i \frac{h\nu_i}{[\exp(h\nu_i/k_B\{T^* + \Delta T\}) - 1]}, \tag{6}$$

where $E_{ph} = h\nu$ (the energy of the photon). In Eqs. (4) and (6) it is assumed that angular momentum conservation does not constrain either the energy accessible to the R rotational degrees of freedom or the relative kinetic energy of the reaction products.

If Eq. (6) is rewritten in the form

$$f(\Delta T) = \frac{(R-1)}{2} k_B\{T^* + \Delta T\} + k_B\{T^* + \Delta T\} + \sum_i \frac{h\nu_i}{[\exp(h\nu_i/k_B\{T^* + \Delta T\}) - 1]} - (E^* + E_{ph}) \tag{7}$$

then the Newton–Raphson approximation

$$\Delta T_{i+1} = \Delta T_i - f(\Delta T_i)/f'(\Delta T_i) \tag{8}$$

can be used to find ΔT in the limit $f(\Delta T_i)/f'(\Delta T_i) \rightarrow 0$, where

$$f'(\Delta T_i) = \frac{\partial f(\Delta T_i)}{\partial \Delta T_i} \tag{9}$$

and ΔT_i and ΔT_{i+1} refer to the results of successive interations. Typically, Eq. (8) converges to within 0.01% in less than five iterations. The new temperature of the cluster ion is then $T^* + \Delta T$ and the associated kinetic energy release should be

$$\varepsilon_{tph} = k_B\{T^* + \Delta T\}. \tag{10}$$

In the approach outlined above, the theory is used to calculate an increase in kinetic energy that should result from the addition of a fixed amount of energy to each ion. Thus, even if the estimates of T^* [Eq. (5)] are not strictly correct, the route to ΔT via the quantum mechanical partition function for a collection of harmonic oscillators, should rescale each kinetic energy release from ε_t to ε_{tph} by the correct magnitude. The broader implications of this approach are that within the time scale of a reaction (which in this case is the loss of SF_6) all or part of the energy of the photon is equipartioned among the available degrees of freedom in the cluster. In effect we are attempting to "warm up" the clusters and use kinetic energy release as a measure of the efficiency of that process.

4. Results and discussion

We begin with a brief summary of those properties of SF_6 which are responsible for the success of this series of experiments, where we have been able to undertake an extensive study of the photofragmentation spectra of single chromophores in association with size-selected cluster ions [4–8]. The general approach requires generating heterogeneous clusters of the form YX_n, for which the ionisation energy (IE) of the chromophore Y is greater than that of either the cluster, X_n or a single constituent. Under these circumstances, the mixed cluster may be ionised in the knowledge that the charge will reside on X_n; the implication being that the spectroscopy of a neutral cluster-bound chromophore can be studied and, at the same time, the presence of a charge used to size-select individual species. With the present constituents, sulpher hexafluoride (IE = 13.5–15 eV [11–13]) and benzene (IE = 9.2 eV), the large difference in ionisation energies ensures that the charge will be located on the cluster component.

Neutral SF_6 has an infrared active, triply degenerate (T_{1u}) vibrational mode (ν_3) which gives a very strong absorption feature in the gas phase at 948 cm^{-1} and falls within the 10P branch of a line-tuneable CO_2 laser. The infrared excitation of the $SF_6.(C_6H_6)_n^+$ cluster ion series, as a function of laser wavelength, has been the subject of an earlier study where results were presented for n in the range 1–25 [4]. By monitoring reaction (2) as a function of cluster size and laser wavelength, it was possible to determine individual infrared (IR) absorption profiles by summing fragment ion intensities. Two examples are shown in Fig. 1, where profiles have been recorded for $SF_6.(C_6H_6)_3^+$ and $SF_6.(C_6H_6)_5^+$. The general shape and position of each absorption profile is characteristic of the ν_3 mode in neutral SF_6, and similar profiles have been recorded for $SF_6.(CO_2)_n^+$ [5], $SF_6.(NO)_n^+$ [6], $SF_6.Ar_n^+$ [7], and $SF_6.Kr_n^+$ [8]. In addition, Scoles and co-workers have observed similar absorption features in neutral SF_6Ar_n clusters [9,14], and a detailed theoretical analysis of this work has been presented by Eichenauer and Le Roy [15]. In particular, these authors provide a description of the interactions responsible for perturbing the ν_3 vibrational mode in SF_6 when the molecule is trapped in and on a cluster. Benzene and benzene clusters also exhibit an infrared absorption which falls within the 10P branch of the CO_2 laser [16], however, the infrared mode(s) responsible has a much smaller infrared transition dipole than that seen in SF_6, and the frequency maximum is shifted well away from the prominent laser lines used in these experiments.

Laboratory-frame kinetic energy profiles were recorded for $SF_6.(C_6H_6)_n^+$ cluster ions for the range n = 2–8, and with the laser operating on the 10P18 transition at 945.98 cm^{-1}. Due to small shifts in the infrared absorption profiles across the size range under study, the above frequency proved to be most appropriate. From Secs. 2 and 3, it follows that each

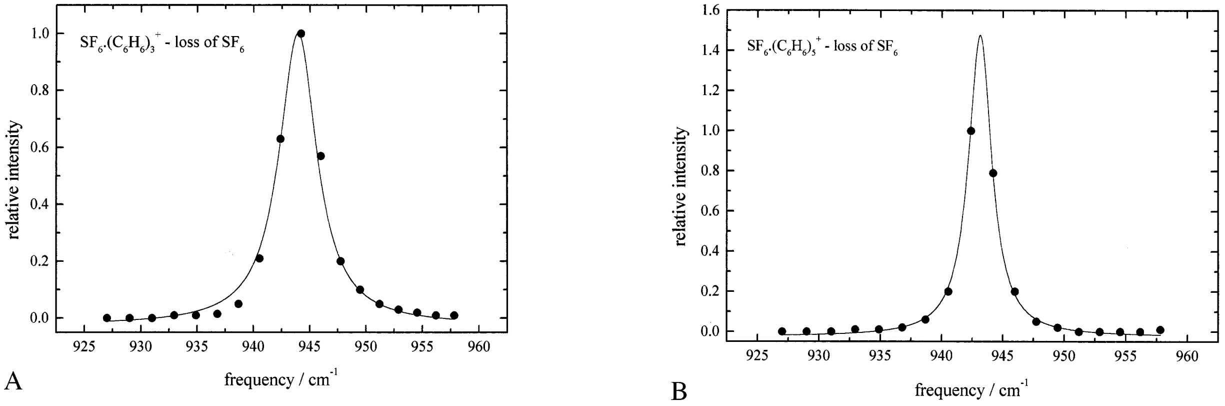

Fig. 1. Two examples of infrared absorption profiles recorded by summing all fragment ion intensities as a function of laser wavelength. The points are the experimental data and the solid line is a fitted Lorentzian profile.

photofragmentation experiment at the above laser frequency, consists of the following steps. A metastable peak profile for the unimolecular decay of a size-selected $SF_6.(C_6H_6)_n^+$ cluster ion is recorded and, from Eqs. (1) and (2), the measured kinetic energy release, ε_t, is used to establish T^* and E^*. The cluster ion is then photoexcited and the corresponding photofragment peak profile recorded in order to measure any increase in kinetic energy brought about as a result of additional internal energy contributed by the photon. Figs. 2 and 3 show examples of fragmentation peak profiles, plotted as a function of the laboratory frame kinetic energy and recorded following the decay of $SF_6.(C_6H_6)_n^+$ from both metastable and laser excitation [reaction (2) in each case].

To extract accurate kinetic energy releases all laboratory-frame profiles, both metastable and photoinduced, were modeled using a Monte Carlo simulation program which provides a complete numerical description of the apparatus [17]. No a priori assumption is made in the simulation regarding the nature of the kinetic energy distribution required to fit the experimental data, i.e. Rice–Ramsberger–Kassel–Marcus (RRKM) or phase space theory; the purpose of the simulation is merely to determine an accurate value for the average energy release. The simulated results are presented in Figs. 2 and 3 as solid lines, together with the experimental data points.

The centre of mass kinetic energy releases extracted from the metastable peak profiles are given in Table 1. The data show a gradual increase as a function of cluster size, which is similar to the pattern

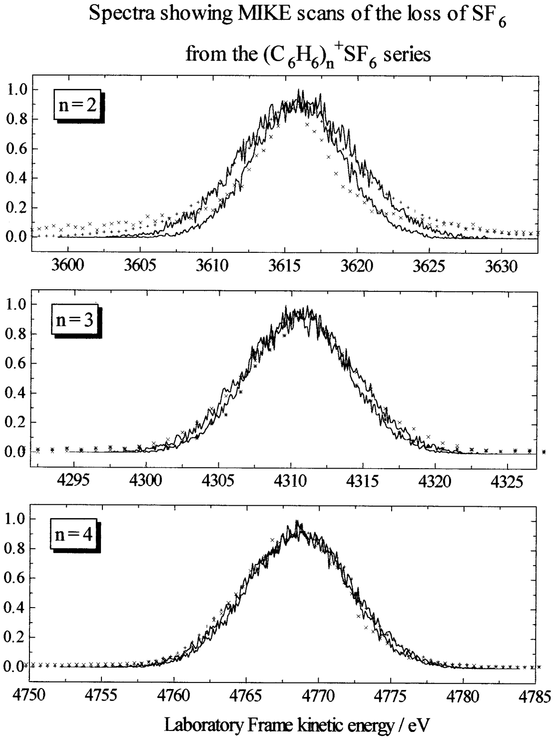

Fig. 2. Laboratory-frame kinetic energy measurements for reaction (2) following the metastable and photoinduced fragmentation of $SF_6.(C_6H_6)_2^+$–$SF_6.(C_6H_6)_4^+$ cluster ions. The symbols denote experimental data and the computer simulated fits are shown as solid lines.

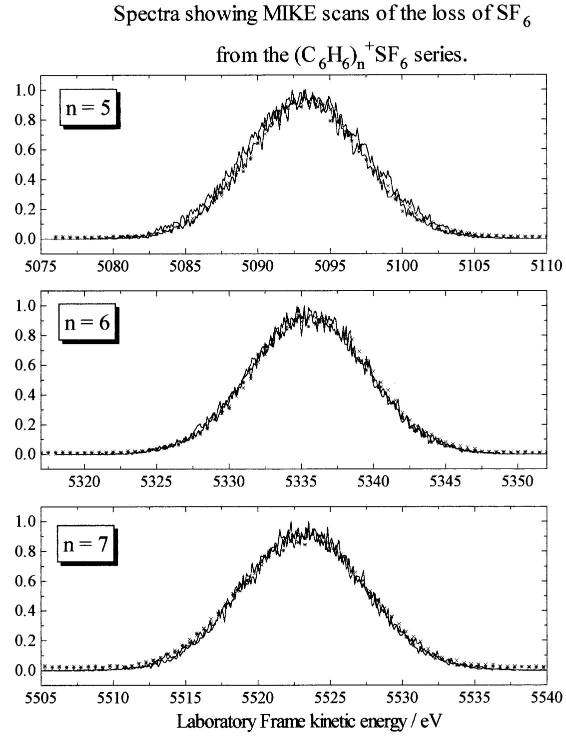

Fig. 3. As for Fig. 2, but for cluster ions in the range $SF_6.(C_6H_6)_5^+$–$SF_6.(C_6H_6)_7^+$.

observed previously for metastable kinetic energy measurements on Ar_n^+ [18,19] and $(CO_2)_n^+$ [20]. This behaviour has been attributed to a combination of instrumental effects and an increase in the internal energy content of the cluster ions as a function of size [18–20]. The principal factor influencing the internal energy content of an ion that fragments in the 2ffr of a sector mass spectrometer, is the lifetime window, which is of the order of 10^{-4} s. For an ion with a small number of degrees of freedom, the excess energy has to be very low if it is to live long enough to reach the 2ffr and, as their size increases, ions which fit within the lifetime window are able to accommodate more energy. However, these changes do not necessarily imply a linear increase in the kinetic energy release because larger ions have more degrees of freedom over which energy can be partitioned.

Table 1
Experimental kinetic energy releases (ε_t and $\varepsilon_{t\text{ph}}$) recorded for the metastable and laser-induced decay of $SF_6.(C_6H_6)_n^+$ cluster ions; the CO_2 laser wavelength was 947 cm^{-1}

n	Metastable (ε_t/meV)	Laser ($\varepsilon_{t\text{ph}}$/meV)
2	4.2	6.7
3	5.2	6.6
4	5.9	6.7
5	8.1	9.6
6	9.5	9.4
7	11.0	11.6
8	12.3	12.2

Table 1 also presents the kinetic energy releases recorded following laser-induced fragmentation. The results for small cluster ions follow the expected trend, i.e. $\varepsilon_{t\text{ph}}(CO_2 \text{ laser}) > \varepsilon_t(\text{metastable})$; however, beyond $n = 5$ the laser and metastable results converge rapidly. This is most likely due to the fact that the energy from each photon represents a diminishing fraction of the total internal energy available for fragmentation.

Eqs. (4)–(10) have been used to calculate the kinetic energy releases based on the assumption that some or all of the energy available from the photon is equipartioned among all the internal degrees of freedom. It is assumed that prior to photon excitation any internal energy the ions might have received as a result of electron impact ionisation, is completely randomised. The reason being that these ions are approximately 10^{-4} s “old” when they reach the point where they interact with the laser, which is more than sufficient time for complete energy randomisation. Furthermore, the ions will have undergone numerous evaporative steps whilst in the ion source, and therefore form part of an “evaporative ensemble” for which a temperature can be defined [21–24].

It is evident from the calculated results presented in Fig. 4 that the assumption of complete photon energy randomisation, predicts energy releases that are much larger than those recorded in the experiment. This observation is particularly true of those measurements made for the smaller clusters containing 2–4 benzene molecules, and is also consistent with previous results [1,2]. At larger values of n the distinction between experiment and theory is less marked, but this probably reflects the fact that the

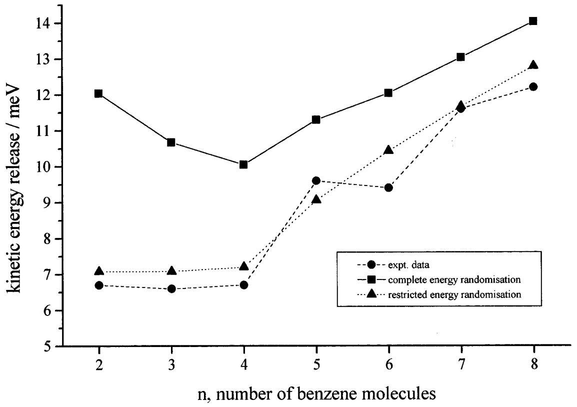

Fig. 4. Comparison between the experimental centre of mass kinetic energy releases and results calculated assuming either complete or partial photon energy randomisation. The assumptions behind both calculations are discussed in the text.

magnitude of the heat sink increases quite rapidly as a function of cluster size. Also presented in Fig. 4 are results calculated on the assumption just ~300 cm^{-1} of the photon's energy is randomised to the benzene cluster. The agreement with experiment is now excellent, and in particular, the results match the experimental trend seen in the smaller clusters. For the larger clusters ($n \geq 5$) the uncertainties in the experimental data are such that the evidence for partial energy randomisation is less conclusive. The calculated kinetic energy releases are also given in Table 2.

These results are consistent with those recorded earlier for small $SF_6.(NO)_n^+$ and $SF_6.Ar_n^+$ cluster ions [1,2], and support the conclusion that, following photoexcitation, vibrational energy in the ν_3 mode undergoes partial relaxation to either the ν_2 or ν_4 modes. The energy difference is then partitioned to the remainder of the cluster and some fraction appears as kinetic energy release. In two gas phase studies involving CO_2 laser excitation [25,26], it was observed that collisional relaxation from the ν_3 ($v = 1$) state of SF_6 can proceed through a rapid *V–V* transfer process involving either the ν_4 vibrational level [26] at 625 cm^{-1} or the ν_6 level [25] at 363 cm^{-1}. In addition, the latter state was found to act as a bottleneck with subsequent *V–T* energy transfer acting as a rate-determining step to total relaxation of the SF_6 molecule [25]. A similar conclusion regarding the relaxation mechanism was reached following a matrix-isolation study of SF_6 by Boissel et al. [27]. Relaxation of the excited molecule was followed as a function of time in matrices consisting of N_2, Ne, Ar, Kr, and Xe. The results were interpreted in terms of a relaxation process which proceeds via a rapid cascade (nanosecond time scale) from $\nu_3 \rightarrow \nu_6$, to be followed by a much slower decay from the ν_6 vibrational level. Measured time scales for the subsequent dissipation of ν_6 ($v = 1$) into the lattice phonon modes ranged from <10 ns (N_2) to 1850 ns (Xe). Relaxation times in benzene could be longer than those seen in the inert gases, in which case they could approach the duration of the experiment (~10^{-5} s). The results of Bates et al. [25] would certainly provide some justification for selecting ν_4 as the intermediate state for the purposes of accounting for the restricted relaxation step identified here and in other related experiments [1,2].

Table 2
Summary of the temperatures derived for the $SF_6.(C_6H_6)_n^+$ ions and the predicted kinetic energy releases (ε_{tph}) for the photodissociation channel

n	T*/K	ΔT/K	ε_{tph}/meV[a]
2	49	33	7.1
3	59	23	7.1
4	66	17	7.2
5	94	12	9.1
6	110	10	10.4
7	128	8	11.6
8	143	6	12.7

[a] Kinetic energy releases calculated from the restricted energy randomisation model presented in the text.

From the calculations it is also possible to determine an initial temperature (T*) for the clusters and a temperature increase (ΔT) resulting from photoexcitation, and these results are given in Table 2 and plotted in Fig. 5. Compared with previous results [1,2], the initial temperatures are, as expected, significantly larger than those determined for the smaller heat sinks of argon and nitric oxide. Likewise, the increases in temperature, observed as a result of photoexcitation, are considerably smaller for benzene than for the other two examples [1,2].

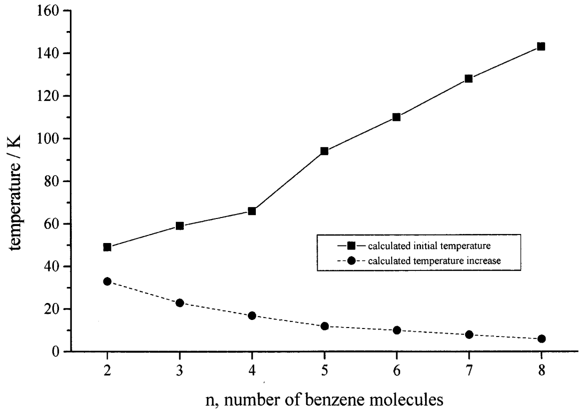

Fig. 5. Calculated initial temperatures for the $SF_6.(C_6H_6)_n^+$ cluster ions plotted as a function of cluster size. Also shown are temperature increases predicted as a result of photoexcitation followed by partial vibrational energy relaxation.

5. Conclusion

Results have been presented of kinetic energy release measurements following the photoexcitation of small $SF_6.(C_6H_6)_n^+$ cluster ions. A comparison between experimental and calculated energy releases for $n \leq 4$ shows evidence of incomplete energy randomisation, in the sense that the excited vibrational mode in SF_6 undergoes only partial relaxation. Consistent with earlier measurements on other mixed cluster systems, the photoexcited mode is found to relax to a vibrational level approximately 300 cm^{-1} lower in energy (either ν_2 or ν_4). The excess energy ($\sim$300 cm^{-1}) is partitioned to the cluster, and as expected, the magnitude of the heat sink has a measurable effect on kinetic energy release when the results from $SF_6.Ar_n$, $SF_6.(NO)_n$, and $SF_6.(C_6H_6)_n$ are compared. In the larger $SF_6.(C_6H_6)_n$ clusters, experimental uncertainties mean that the evidence for partial energy relaxation is not so conclusive.

Finally, it was concluded from an earlier spectroscopic study of $SF_6.(C_6H_6)_n^+$ clusters [4], that SF_6 occupied a surface site, which was probably responsible for the continued prominence of reaction (2), even in the very large clusters. However, we might also have expected the very specific nature of the photodissociation channel to have been reflected in the energy release process. The fact that the complexes appear to participate in the restricted energy randomisation process, suggests that subtle differences in the unimolecular rate constant as a function of internal energy may be responsible for the observed photofragmentation pattern.

Acknowledgements

The authors would like to thank EPSRC for the award of a studentship to one of the authors (S.A.) and Professor A. Carrington for the loan of a CO_2 laser.

References

[1] S. Atrill, A. Mouhandes, J.F. Winkel, A. Goren, A.J. Stace, Faraday Discuss. 102 (1995) 339.
[2] S. Atrill, A.J. Stace, J. Chem. Phys., in press.
[3] C.E. Klots, J. Chem. Phys. 58 (1973) 5364.
[4] A.B. Jones, R. Lopez-Martens, A.J. Stace, J. Phys. Chem. 99 (1995) 6333.
[5] A.B. Jones, C.A. Woodward, J.F. Winkel, A.J. Stace, Int. J. Mass Spectrom. Ion Process. 133 (1994) 83.
[6] J.F. Winkel, A.B. Jones, C.A. Woodward, D.A. Kirkwood, A.J. Stace, J. Chem. Phys. 101 (1994) 9436.
[7] J.F. Winkel, C.A. Woodward, A.B. Jones, A.J. Stace, J. Chem. Phys. 103 (1995) 5177.
[8] S. Atrill, A.J. Stace (submitted).
[9] S. Goyal, D.L. Schutt, G. Scoles, Acc. Chem. Res. 26 (1993) 123.
[10] R.G. Cooks, J.H. Beynon, R.M. Caprioli, G.R. Lester, Metastable Ions Elsevier, Amsterdam, 1973.
[11] E.R. Fisher, B.L. Kickel, P.B. Armentrout, J. Chem. Phys. 97 (1992) 4859.
[12] A.J. Stace, A.B. Jones, J.F. Winkel, C.A. Woodward, J. Phys. Chem. 97 (1993) 11 363.
[13] M. Evans, C.Y. Ng, C.-W. Hsu, P. Heimann, J. Chem. Phys. 106 (1997) 978.
[14] S. Goyal, G.N. Robinson, D.L. Schutt, G. Scoles, J. Phys. Chem. 95 (1991) 4186.
[15] D. Eichenauer, R.J. Le Roy, J. Chem. Phys. 88 (1988) 2898.
[16] A.J. Stace, D.M. Bernard, J.J. Crooks, K. Reid, Mol. Phys. 60 (1987) 671.
[17] J.E. Upham, Ph.D. thesis, University of Sussex, 1991.
[18] A.J. Stace, J. Chem. Phys. 85 (1986) 5774.
[19] C.A. Woodward, A.J. Stace, J. Chem. Phys. 94 (1991) 4234.
[20] A.J. Stace, A.K. Shukla, Chem. Phys. Lett. 85 (1982) 157.
[21] C.E. Klots, J. Phys. Chem. 92 (1988) 5864.
[22] C.E. Klots, J. Chem. Phys. 90 (1989) 4470.
[23] C.E. Klots, Z. Phys. D 20 (1991) 105.
[24] C.E. Klots, Z. Phys. D 21 (1991) 335.
[25] J.I. Steinfeld, I. Burak, D.G. Sutton, A.V. Nowak, J. Chem. Phys. 52 (1970) 5421.
[26] R.D. Bates, J.K. Knudston, G.W. Flynn, A.M. Ronn, Chem. Phys. Lett. 8 (1971) 103.
[27] P. Boissel, B. Gauthier-Roy, L. Abouaf-Marguin, Chem. Phys. 119 (1988) 419.